The EMBO Journal Vol.17 No.22 pp.6608–6621, 1998

Phosphorylation-dependent and constitutive activation of Rho proteins by wild-type and oncogenic Vav-2

Kornel E.Schuebel, Nieves Movilla, José Luis Rosa[1] and Xosé R.Bustelo[2]

Department of Pathology, State University of New York at Stony Brook, University Hospital, Level 2, Room 718-B, Stony Brook, NY 11794-7025, USA

[1]Present address: Unidad de Bioquímica (4178), Facultad de Medicina, Campus de Bellvitge, Universidad de Barcelona, C/ Feixa Llarga s/n, 08907 Hospitalet (Barcelona), Spain

[2]Corresponding author
e-mail: xbustelo@path.som.sunysb.edu

We show here that Vav-2, a member of the Vav family of oncoproteins, acts as a guanosine nucleotide exchange factor (GEF) for RhoG and RhoA-like GTPases in a phosphotyrosine-dependent manner. Moreover, we show that Vav-2 oncogenic activation correlates with the acquisition of phosphorylation-independent exchange activity. *In vivo*, wild-type Vav-2 is activated oncogenically by tyrosine kinases, an effect enhanced further by co-expression of RhoA. Likewise, the Vav-2 oncoprotein synergizes with RhoA and RhoB proteins in cellular transformation. Transient transfection assays in NIH-3T3 cells show that phosphorylated wild-type Vav-2 and the Vav-2 oncoprotein induce cytoskeletal changes resembling those observed by the activation of the RhoG pathway. In contrast, the constitutive expression of the Vav-2 oncoprotein in rodent fibroblasts leads to major alterations in cell morphology and to highly enlarged cells in which karyokinesis and cytokinesis frequently are uncoupled. These results identify a regulated GEF for the RhoA subfamily, provide a biochemical explanation for *vav* family oncogenicity, and establish a new signaling model in which specific Vav-like proteins couple tyrosine kinase signals with the activation of distinct subsets of the Rho/Rac family of GTPases.

Keywords: GDP–GTP exchange factors/phosphorylation/Rac/Rho/Vav family

Introduction

The GTP-binding proteins of the Rho/Rac family participate in coordinated cellular responses to extracellular stimuli (for a review see Van Aelst and D'Souza-Chorey, 1997; Hall, 1998). Their action is essential to promote the formation of cytoskeletal structures, the activation of kinase cascades and the induction of nuclear responses required for both developmental and proliferative decisions (Van Aelst and D'Souza-Chorey, 1997; Hall, 1998). Members of this family can be grouped into three classes according to amino acid sequence similarities. The first subfamily is composed of four Rac proteins (Rac-1, Rac-2, Rac-3 and RhoG). Some of these proteins promote the activation of protein kinases such as PAK, c-Jun N-terminal kinase (JNK) and $p38^{MAPK}$. They are also involved in the activation of other independent pathways regulating membrane ruffling and cell proliferation (Van Aelst and D'Souza-Chorey, 1997; Hall, 1998). The second subfamily, Rho, includes RhoA, RhoB, RhoC, RhoD, RhoE and TTF proteins. Of these, RhoA has been characterized extensively and shown to be involved in cell transformation, formation of stress fibers and focal adhesions, and in the stimulation of protein kinases such as PKN and $p160^{Rock}$ (Van Aelst and D'Souza-Chorey, 1997). Finally, the third subfamily is composed of TC10 and the two isoforms of the Cdc42 protein. In this subfamily, Cdc42 was shown to be involved in the activation of JNK, PAK and $p38^{MAPK}$ as well as in the formation of filopodia in the plasma membrane (Van Aelst and D'Souza-Chorey, 1997; Hall, 1998).

The activation and deactivation cycle of most Rho proteins is regulated by the differential binding of guanosine nucleotides (for a review see Boguski and McCormick, 1993). In quiescent cells, these GTPases are in an inactive state maintained by the presence of bound GDP molecules. Stimulation of cells via a number of extracellular stimuli leads to the exchange of GDP by GTP molecules, a transition that allows the release of inhibitory molecules from the GTPases (GDP dissociation inhibitors), the translocation of the GTP-binding proteins to the plasma membrane and the acquisition of a tertiary conformation optimal for the binding of their effector molecules (Boguski and McCormick, 1993). The exchange of guanosine nucleotides on these GTPases is catalyzed by guanosine nucleotide exchange factors (GEFs) (Boguski and McCormick, 1993). To date, two different families of Rho GEFs have been identified that differ in the structure of their catalytic domains. The first group is composed of Rho GDP dissociation stimulators (GDS), a family of proteins distantly related to the Cdc25 homology regions present in Ras GEFs (Boguski and McCormick, 1993). GDSs work at stoichiometric concentrations and have a rather broad catalytic specificity, being active on prenylated K-Ras, Rho and Rap proteins (Boguski and McCormick, 1993). The second subset of Rho activators comprises an extensive number of enzymes containing Dbl-homology (DH) domains with catalytic activity exclusively directed towards Rho/Rac GTPases (for a review see Cerione and Zheng, 1996). The majority of these GEFs are highly transforming when overexpressed either as wild-type or truncated proteins (Cerione and Zheng, 1996), a property that highlights their importance as regulators of mitogenic processes.

Although Rho GEFs have been characterized extensively both biochemically and oncogenically, little information is available regarding the mechanism by which they become activated during signal transduction. To date, the

best example for the participation of a DH-containing protein in receptor-mediated cell signaling is the product of the *vav* proto-oncogene, a protein preferentially expressed in the hematopoietic system (for a review see Bustelo, 1996). In addition to the DH and pleckstrin homology (PH) regions commonly found in Rho/Rac GEFs, Vav contains other structural motifs, including a calponin-homology (CH) region, an acidic domain (AD), a zinc finger butterfly motif, two SH3 regions and one SH2 domain (Bustelo, 1996). Vav becomes tyrosine phosphorylated during the signaling of many receptors with intrinsic or associated protein tyrosine activity (Bustelo, 1996), and binds to a number of signaling molecules via its SH2 and SH3 domains (Bustelo, 1996). Recently, biochemical experiments have demonstrated that the phosphorylation of Vav on tyrosine residues leads to the activation of its GDP/GTP exchange activity towards Rac-1 (Crespo *et al*., 1997). In good agreement with such observations, it has been shown that several elements of the Rac-1 pathway, including Rac-1 itself and JNK, are activated by wild-type Vav protein upon co-transfection with protein tyrosine kinases (Crespo *et al*., 1997; Teramoto *et al*., 1997). More recently, Han *et al*. (1998) have shown that the activity of phosphorylated Vav can be enhanced further by the binding to the Vav PH domain of products of the phosphatidylinositol 3-kinase. Vav appears, therefore, to be an essential mediator of mitogenic and antigenic signals, providing a direct connection between membrane-derived signals and the activation of the Rac-1 pathway.

Interestingly, Vav appears to be a member of a new family of signal transduction molecules highly conserved during evolution. Thus, a *vav*-related gene was identified recently in *Caenorhabditis elegans* during the characterization of the genome of this nematode. The *C.elegans* Vav-like protein lacks the two C-terminal SH3 domains but maintains all the other structural domains present in the mammalian counterpart (Bustelo, 1996). In addition, a new protein (Vav-2) with the same arrangement of structural domains as Vav has been identified both in human and mouse (Henske *et al*., 1995; Schuebel *et al*., 1996). In spite of their structural similarity, Vav and Vav-2 differ in several biological properties. For example, Vav-2 displays a ubiquitous pattern of expression during both embryonic and adult mouse stages (Schuebel *et al*., 1996). Moreover, Vav-2 requires a more extensive deletion of the N-terminus than Vav to become oncogenically active (Schuebel *et al*., 1996). Perhaps more importantly, it has been shown that the expression of the *vav* and *vav-2* oncogenes leads to different types of morphological transformation in rodent fibroblasts (Schuebel *et al*., 1996), a result that suggests that they may work through similar, but not identical, signal transduction pathways. Thus, the discovery of new Vav-like proteins has given further relevance to the role of this protein family in cell signaling and, in addition, has raised new functional questions such as those regarding the type(s) of mechanism(s) of activation and the functional redundancy of the different Vav family members.

In order to characterize the function of this new member of the Vav family in more detail, we have investigated the biochemical and biological properties of both the wild-type and oncogenic forms of Vav-2. Using GDP/GTP exchange reactions, we show here that wild-type Vav-2 is a phosphorylation-dependent GDP/GTP exchange factor that targets a subset of GTP-binding proteins overlapping, but not identical to, those engaged by Vav. Moreover, we demonstrate that Vav-2 transformation is mediated by the expression of a constitutively active protein that leads to morphological changes different from those induced by the Vav oncoprotein. Hence, these results identify a phosphorylation-dependent RhoA subfamily GEF, establish a general mechanism by which Vav family members achieve full oncogenic activity, and suggest a new signaling pathway in which membrane receptors will turn on distinct GTPase pathways via the stimulation of different members of the Vav family.

Results

The Vav-2 oncoprotein induces morphological changes in rodent fibroblasts

We have shown previously that the expression of *vav* and *vav-2* oncogenes in NIH-3T3 cells leads to the generation of foci of different morphology. Thus, expression of both the human and mouse *vav* oncogene induces the generation of dense, non-refractile cells that pile up to form mountain-like foci (Coppola *et al*., 1991; Schuebel *et al*., 1996). Instead, the expression of the *vav-2* oncogene leads to the formation of flat foci composed of monolayers of very enlarged and multinucleated cells that are accompanied by clumps of small, rounded, highly refractile cells (Schuebel *et al*., 1996). To verify that these differences are stable in time, several foci of *vav-2*-transformed cells were randomly picked, expanded and purified further by cloning in soft agar. After this step, individual colonies of *vav-2*-transformed cells were expanded to obtain stable *vav-2*-transformed cell lines. The microscopic examination of these cells showed that they had conserved the morphological change previously detected in the cells within the *vav-2* foci. These cell lines are composed of enlarged and multinucleated cells (Figure 1B, C and F–H), small flat cells, and small and refractile rounded cells whose presence becomes more apparent in confluent cultures (Figure 1B and C). A similar morphological change was observed in cells expressing the *dbl* oncogene (data not shown, Eva and Aaronson, 1985). This phenotype is conserved during multiple passages, although the giant cells are significantly reduced in number after prolonged culture (Figure 1C). Unlike *vav-2*- and *dbl*-expressing cells, *vav*-transformed NIH-3T3 cells display a very low proportion of multinucleated giant cells and the majority of the culture is composed of small flat cells showing frequent membrane ruffling (Figure 1I) that can reach very high cell densities in confluent cultures (Figure 1D). As a negative control, NIH-3T3 cells show a fibroblast-like morphology (Figure 1E) and undergo cell growth arrest after reaching confluency (Figure 1A). As expected, the morphology of both *vav*- and *vav-2*-transformed cells is also quite different from that induced by other unrelated exchange factors, such as Ras GRF, a Ras- and R-Ras-specific GDP/GTP exchange factor (Figure 1J). The morphologies of *vav*- and *vav-2*-transformed cells were observed in six independently cloned cell lines (data not shown).

The morphological transformation induced in NIH-3T3 cells by Vav family proteins results in marked changes in

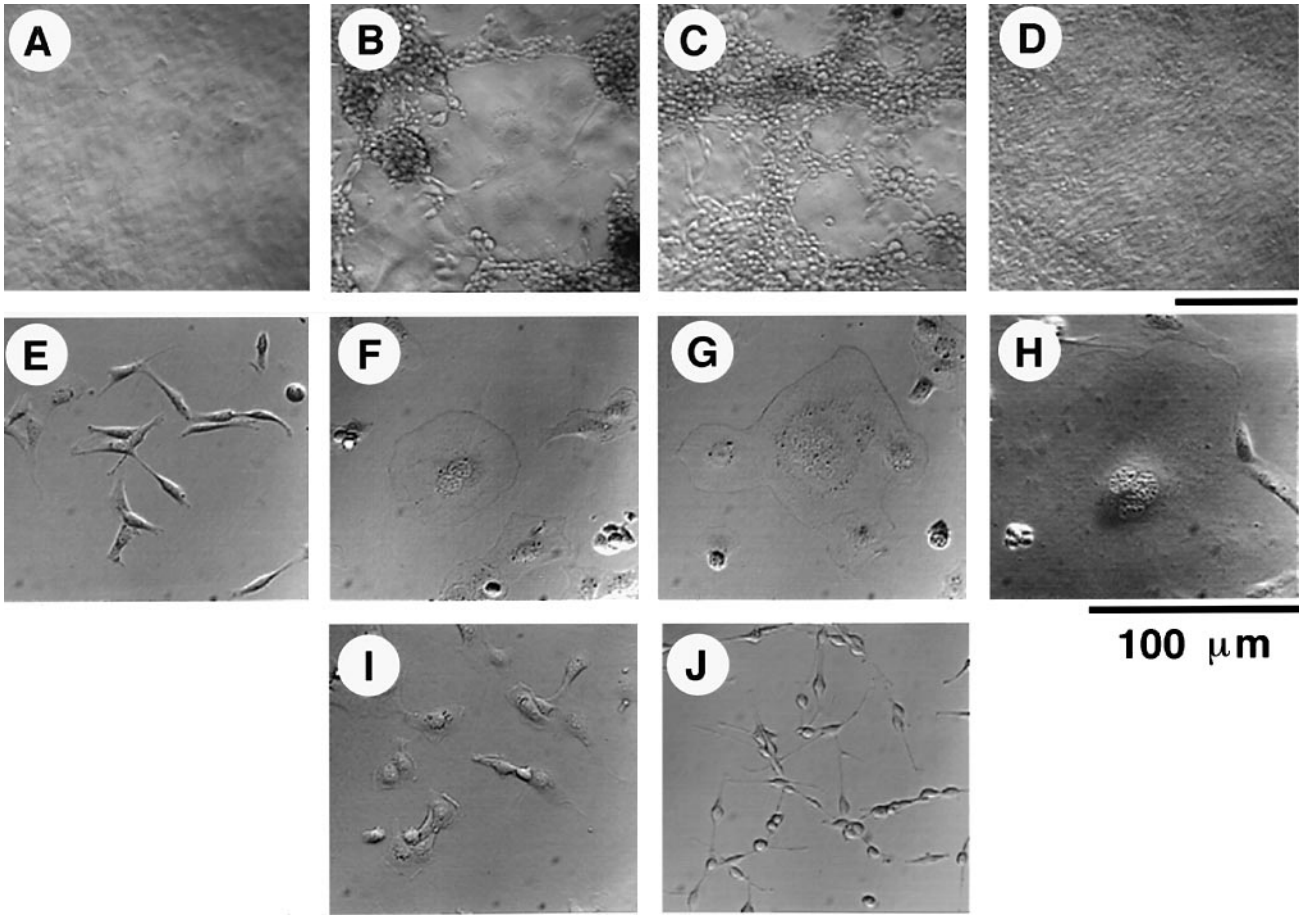

Fig. 1. Morphology of *vav-2*- and *vav*-transformed cells. Confluent (A–D) or subconfluent (E–J) cultures of parental NIH-3T3 cells (**A** and **E**) and established cell lines expressing the mouse *vav-2* oncogene at early (**B** and **F–H**) or after 10 passages (~1 month of culture; **C**), the mouse *vav* oncogene (**D** and **I**) or the farnesylated Cdc25 domain of the rat Ras GRF protein (**J**) were observed under the microscope using Nomarski optics. The scale bars for (A–D) and (E–J) are below (D) and (H), respectively.

the cytoskeleton. Thus, while exponentially growing NIH-3T3 cells show the presence of thin bundles of F-actin in the form of stress fibers (Figure 2A), the expression of the *vav* oncogene leads to a general disruption of stress fibers and to a preferential localization of actin molecules in peripheral membrane structures (Figure 2B). In contrast, expression of the Vav-2 oncoprotein in the same cell background induces the formation of abundant stress fibers in the giant cells (Figure 2C–E). These stress fibers display a parallel distribution in the majority of *vav-2*-transformed cells (Figure 2C and D) although, occasionally, adopt a radial configuration (Figure 2E). The co-staining of these cells with anti-vinculin antibodies revealed that many of the *vav-2*-transformed cells contain thick and long focal adhesion plaques that generally co-localize with the distal tips of the actin fibers (Figure 2F–H). In contrast to the enlarged cells, the morphology of the *vav-2*-transformed cells of normal size was more heterogenous, including the presence of flat cells with stress fiber distributions similar to those discussed above as well as flat or rounded cells showing a total absence of stress fibers and focal adhesions (Figure 2C and F, and E and H). Under these culture conditions, no filopodia were observed in either *vav*- or *vav-2*-transformed cells (Figures 1 and 2). The change in the cytoskeleton in *vav*- and *vav-2*-transformed cells appears to be restricted to the actin network, as other structures such as tubulin microfilaments showed no alteration in those cells (Figure 2I–K). Taken together, these results indicate that the constitutive expression of Vav and Vav-2 oncoproteins induces different morphological changes in rodent fibroblasts, suggesting that their signaling pathways are not identical.

Vav-2 is a phosphorylation-dependent guanosine nucleotide exchange factor for the RhoA subfamily

The different morphology of *vav*- and *vav-2*-transformed cells led us to investigate the catalytic specificity of Vav-2 towards GTP-binding proteins of the Rho family. To this end, we first generated a baculovirus capable of expressing the full-length mouse Vav-2 protein after infection of *Spodoptera frugiperda* (Sf9) cells. To facilitate the recovery of the protein from the total cellular extracts, we included a stretch of polyhistidine residues at the N-terminus of the protein to allow its purification by chromatography onto nickel beads. This method allowed the efficient purification of full-length Vav-2 protein free of other protein contaminants as determined by Coomassie Blue staining of SDS–polyacrylamide gels (Figure 3A). Since the activity of Vav is dependent on tyrosine phosphorylation (Crespo *et al.*, 1997), the purified Vav-2 protein was then incubated with the protein tyrosine kinase Lck in the presence of ATP, a treatment that leads to optimal Vav-2 phosphorylation as determined by *in vitro* kinase assays in the presence of [γ-^{32}P]ATP (Figure 3B).

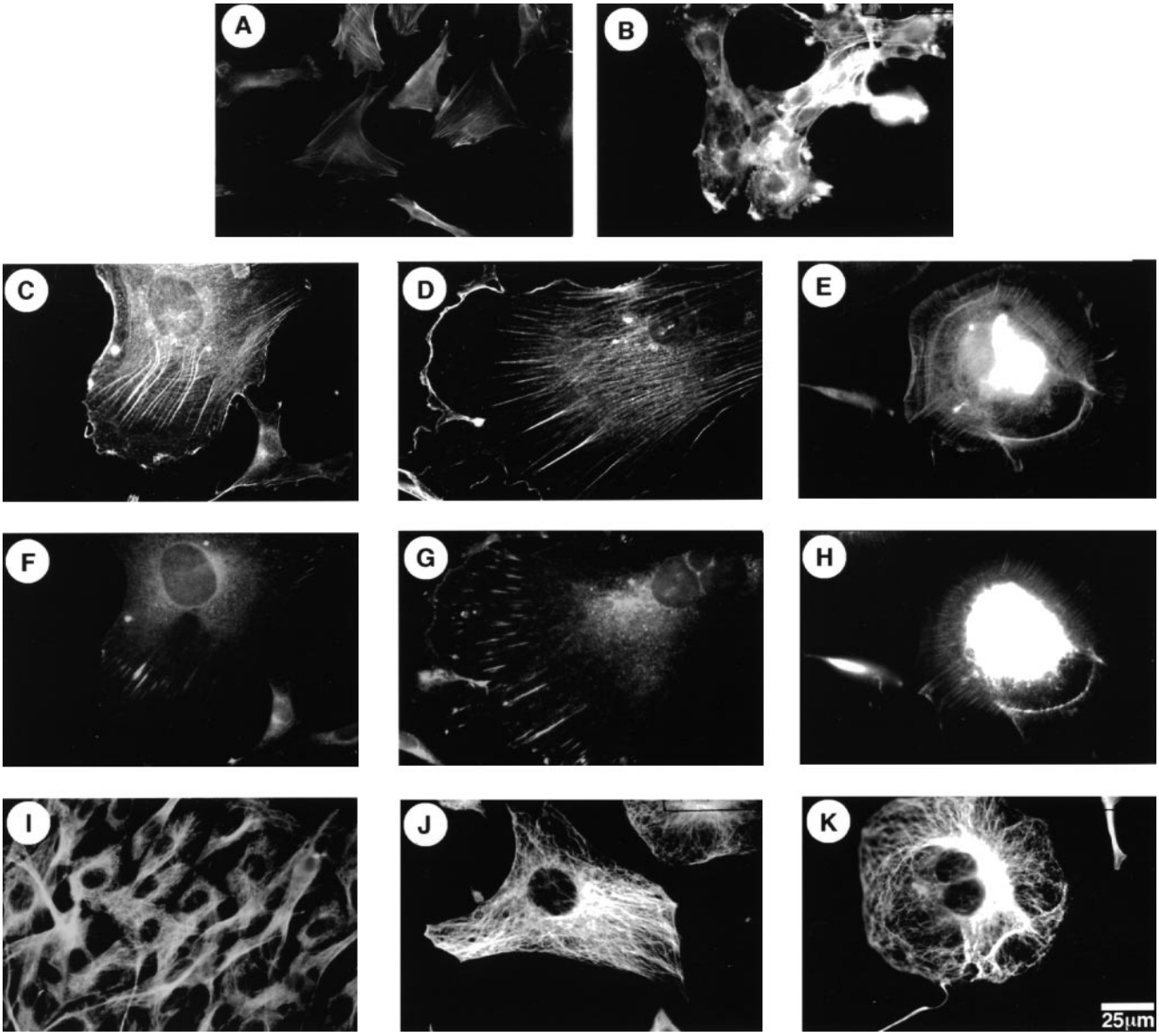

Fig. 2. Cytoskeletal organization of *vav-2*-transformed cells. NIH-3T3 cells (**A** and **I**), *vav*- (**B**) and *vav-2*- (**C–H**, **J** and **K**) transformed cells were submitted to incubations with FITC-labeled phalloidin (A and B–E), or antibodies to either vinculin (F–H) or α-tubulin (I–K), as indicated in Materials and methods. (C and F), (D and G) and (E and H) represent the same cell co-stained with phalloidin and anti-vinculin antibodies.

Next, we purified several representative members of the Rho family as GST fusion proteins to be used as substrates by using a standard bacterial expression system (Figure 3C). After purification, the activity of these proteins was demonstrated by testing their ability to hydrolyze [α-^{32}P]GTP into [α-^{32}P]GDP (Figure 3D).

The exchange activities of the non-phosphorylated and phosphorylated versions of Vav-2 were then determined by measuring their ability to enhance the incorporation of [^{35}S]GTP-γS into GTPases representative of the three branches of the Rho/Rac family (Rac-1, RhoA and Cdc42). As shown in Figure 4A (left panel), the non-phosphorylated version of Vav-2 displays a low, albeit reproducible, exchange activity on RhoA. Most noticeably, phosphorylation of this protein by Lck leads to higher levels of RhoA [^{35}S]GTP-γS binding (Figure 4A, left panel). The stimulation of Vav-2 exchange activity by tyrosine phosphorylation *in vitro* oscillated between 3.5- and 8-fold, depending on the batches of purified Vav-2 protein used in the assays. In contrast to this activity, all Vav-2 batches were inactive towards Rac-1 and Cdc42 (Figure 4A, left panel, and data not shown). To verify that these GTPases were active in this assay, Rac-1 and Cdc42 were submitted to exchange reactions in the presence of either the human Dbl oncoprotein or the non-phosphorylated and phosphorylated versions of mouse Vav. As shown in Figure 4A (right panel), Dbl elicited exchange activity on both RhoA and Cdc42, while phosphorylated Vav did so on Rac-1 (Figure 4A, right panel). Non-phosphorylated Vav induced no detectable nucleotide exchange in any of these GTP-binding proteins (Figure 4A, right panel). These results are in agreement with the catalytic specificity of these GEFs (Zheng *et al*., 1995; Crespo *et al*., 1997), and demonstrate that the lack of activity of Vav-2 towards Rac-1 and Cdc42 is not due to the use of inactive GTPases in these assays.

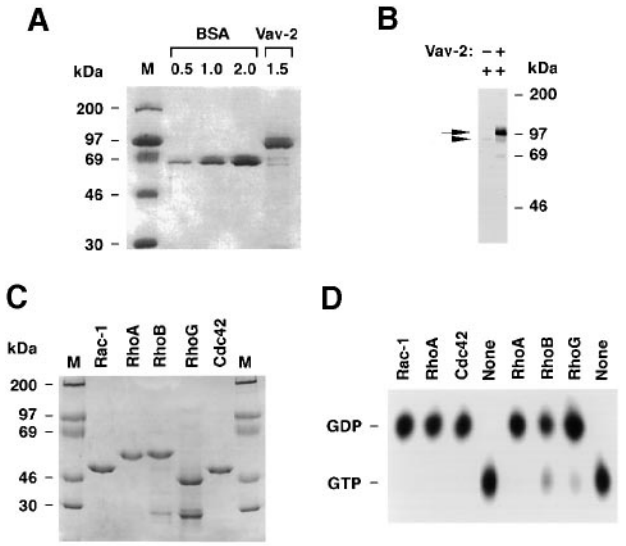

Fig. 3. (**A**) Purification of Vav-2 from Sf9 cells. An aliquot of a preparation of a representative Vav-2 purification were analyzed by SDS–PAGE in the presence of molecular weight markers (M) and increasing concentrations of BSA as standard for concentration. The amount of loaded proteins is given in μg. (**B**) Phosphorylation of wild-type Vav-2 by Lck. *In vitro* kinase reactions were performed with the indicated proteins in the presence of [γ-^{32}P]ATP, separated by SDS–PAGE and submitted to autoradiographic exposure. The migration of Vav-2 and GST–Lck is indicated by an arrow and an arrowhead, respectively. (**C**) Purification of Rho GTP-binding proteins from *E.coli* cells. Aliquots (2 μg) of each purified GST–GTPase were analyzed by SDS–PAGE in the presence of molecular weight markers. (**D**) GTPase activity of purified Rho proteins estimated as described in Materials and methods. The mobility of the ^{32}P-labeled GTP and GDP molecules is indicated on the left.

Time course experiments showed that phosphorylated Vav-2 promotes rapid kinetics of nucleotide exchange on RhoA when compared with either non-phosphorylated Vav-2 or autophosphorylated Lck, confirming that Vav-2 activation occurs in a phosphotyrosine-dependent manner (Figure 4B, left panel). To demonstrate further that this activity represented a bona fide exchange reaction, we also analyzed the ability of Vav-2 proteins to induce the release of [^{3}H]GDP from RhoA in the presence of cold GTP. Tyrosine-phosphorylated Vav-2 enhanced the exchange of nucleotides on RhoA at substoichiometric concentrations under these experimental conditions (Figure 4B, right panel). Taken together, these results indicate that Vav family members share a similar mechanism of activation but display distinct substrate specificity towards members of the Rho/Rac family.

The finding that Vav-2 acted as a phosphorylation-dependent RhoA GEF prompted us to analyze further the specificity of Vav-2 activation. To this end, we first investigated the ability of several protein tyrosine kinases (Lck, Hck and Syk) purified from baculovirus-infected Sf9 cells to induce Vav-2 activation *in vitro*. As shown in Figure 4C, Vav-2 is stimulated efficiently by incubation with these protein tyrosine kinases, as determined by [^{35}S]GTP-γS incorporation assays. Kinase experiments conducted in the presence of [γ-^{32}P]ATP confirmed that these kinases phosphorylate Vav at comparable levels (data not shown). We also analyzed the enzyme specificity of non-phosphorylated and phosphorylated Vav-2 towards additional members of the RhoA subfamily using [^{35}S]GTP-γS binding assays. Phosphorylated Vav-2 was found to be active on RhoA, RhoB and the more distantly related RhoG protein (Figure 4D). In these assays, we found that phosphorylated Vav was active on RhoG and Dbl lysates on all three GTPases (data not shown). These results support the notion that Vav-2 acts as a phosphorylation-dependent GEF with substrate specificity towards RhoG and RhoA subfamily members.

Oncogenic activation of vav-2 leads to the production of a truncated protein with deregulated, phosphorylation-independent exchange activity

The Vav-2 protein is oncogenically activated as a result of an N-terminal truncation that removes both the CH domain and the AD (Schuebel *et al*., 1996). To determine whether this mutation results in a constitutively active Vav-2 protein, we generated a second baculovirus capable of expressing a polyhistidine-tagged version of the Vav-2 oncoprotein in Sf9 cells. After purification from insect cells (Figure 5A), the Vav-2 oncoprotein was subjected to *in vitro* kinase assays in the presence or absence of GST–Lck and then tested for GDP/GTP exchange activity on bacterially expressed Rho family proteins using [^{35}S]GTP-γS incorporation assays. Both the non-phosphorylated and phosphorylated forms of the Vav-2 oncoprotein were active preferentially on RhoA and, to a lesser extent, on RhoB and RhoG GTPases (Figure 5B, left panel). In contrast, both versions of the Vav-2 oncoprotein lacked significant activity on Rac-1 and Cdc42 (Figure 5B, right panel). The Vav-2 oncoprotein was also inactive on Rac-2 protein (data not shown). These experiments indicated, therefore, that the Vav-2 oncoprotein has the same substrate specificity as wild-type Vav-2 but, unlike this protein, its activity is independent of its phosphorylation status. We also performed [^{3}H]GDP release experiments in order to corroborate the de-regulated activity of the Vav-2 oncoprotein. As shown in Figure 5C, the kinetics of guanosine nucleotide exchange induced on RhoA by the non-phosphorylated and phosphorylated forms of the Vav-2 oncoprotein were indistinguishable under these alternative experimental conditions. Based on these results, we conclude that the Vav-2 oncoprotein is active regardless of its phosphorylation state.

Since these experiments could not rule out the possibility that the de-regulated activity of the oncogenic version of Vav-2 was due to high levels of phosphorylation of this protein in insect cells, we investigated the levels of tyrosine phosphorylation of the wild-type and oncogenic Vav-2 proteins in baculovirus-infected Sf9 cells. As shown in Figure 5D, immunoblot analysis indicated that the basal levels of phosphorylation of the Vav-2 oncoprotein in the total cellular lysates obtained from Sf9 cells were significantly lower than those found in its wild-type counterpart, ruling out the possibility that the de-regulated activity of the Vav-2 oncoprotein in our biochemical assays is a consequence of its hyperphosphorylation in insect cells.

Vav family members share a similar mechanism of oncogenic activation

In contrast to Vav-2, it has been shown previously that Vav becomes activated oncogenically upon a partial deletion of

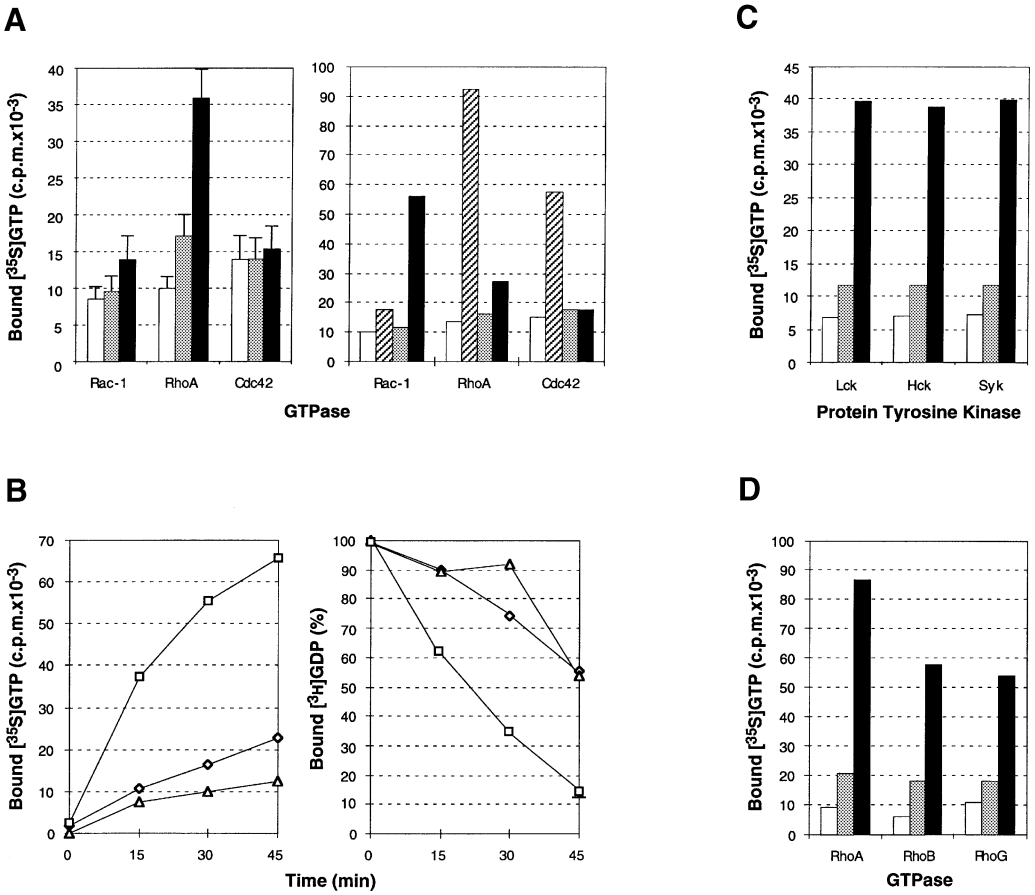

Fig. 4. (**A**) Exchange of Vav-2 on Rho/Rac proteins. Left panel: GDP-loaded GTPases were incubated for 45 min with [^{35}S]GTP-γS in the presence of phosphorylated Vav-2 (black boxes), non-phosphorylated Vav-2 (gray boxes) or autophosphorylated GST–Lck (white boxes). Right panel: exchange of Dbl and Vav on Rho/Rac proteins. Reactions were conducted as above with either autophosphorylated Lck (white boxes), non-phosphorylated Vav (gray boxes), phosphorylated Vav (black boxes) or Dbl (shaded boxes). (**B**) Kinetics of Vav-2 exchange on Rho using [^{35}S]GTP incorporation (left panel) or [^{3}H]GDP release (right panel) assays. RhoA was pre-loaded with either cold GDP (left panel) or [^{3}H]GDP (right panel) and submitted to exchange reactions for the indicated periods of time with autophosphorylated Lck (triangles), non-phosphorylated Vav-2 (diamonds) or phosphorylated Vav-2 (squares). (**C**) Activation of Vav-2 exchange activity by protein tyrosine kinases. GDP-loaded GTPases were incubated with [^{35}S]GTP-γS in the presence of phosphorylated Vav-2 (black boxes), non-phosphorylated Vav-2 (gray boxes) or the indicated autophosphorylated protein tyrosine kinase (white boxes). After 45 min, the incorporation of [^{35}S]GTP-γS onto RhoA was determined as indicated in (A). (**D**) Exchange activity of Vav-2 towards RhoA subfamily members. The indicated GDP-loaded GTPases were submitted to exchange reactions under the conditions indicated in (A). In (A), values represent the mean and standard deviation (SD) of three independent determinations each performed in duplicate. (B, C and D) show a representative experiment of two independent determinations, each performed in duplicate.

the N-terminal CH domain (residues 1–67) (Coppola *et al*., 1990; Katzav *et al*., 1990). However, this oncogenic protein is not totally unregulated, as demonstrated by previous reports showing that the Vav oncoprotein requires phosphorylation for nucleotide exchange *in vitro* (Crespo *et al*., 1997). In order to investigate whether the mechanism of activation of Vav-2 could be generalized to all Vav family proteins, we compared the transforming activity of the wild-type, the originally described Vav oncogenic version (Δ1–67 deletion) (Coppola *et al*., 1991; Katzav *et al*., 1991), and a new version of Vav lacking both the CH domain and the AD (Δ1–187) (Figure 6A) using focus formation assays in rodent fibroblasts. To ensure that all proteins were expressed with similar kinetics, all cDNAs were cloned in pMEX, a mammalian expression vector containing the mouse mammary tumor virus (MMTV) long terminal repeat. Consistent with previous reports (Coppola *et al*., 1991; Katzav *et al*., 1991), we found that the wild-type Vav protein has a very low oncogenic potential (62 foci/μg; Figure 6A, plate 1). The transforming activity of Vav is enhanced 12-fold upon the deletion of the 67 N-terminal amino acids (Figure 6A, plate 2) (Coppola *et al*., 1991; Katzav *et al*., 1991). In the same experiments, the expression in NIH-3T3 cells of the Vav mutant lacking both the CH domain and the AD results in levels of morphological transformation ≈150-fold higher than those found with the wild-type Vav protein (9640 foci/μg; Figure 6A, plate 3). In spite of this higher transforming activity, the foci generated by the Vav(Δ1–187) protein retain the usual morphology found in those derived from the *vav*(Δ1–67) oncogene, and lack the highly multinucleated and enlarged cells that are characteristic of *vav-2*-derived foci (data not shown), suggesting that the different morphologies displayed by *vav*(Δ1–67)- and *vav-2*-transformed cells are not the consequence of different levels of activity of these proteins towards identical substrates.

The detectable transforming activity of wild-type Vav, Vav(Δ1–67) and Vav(Δ1–187) allowed us to study further the dependency of phosphorylation for Vav transformation *in vivo*. To this end, we next tested the transforming activity of mammalian expression vectors encoding versions of

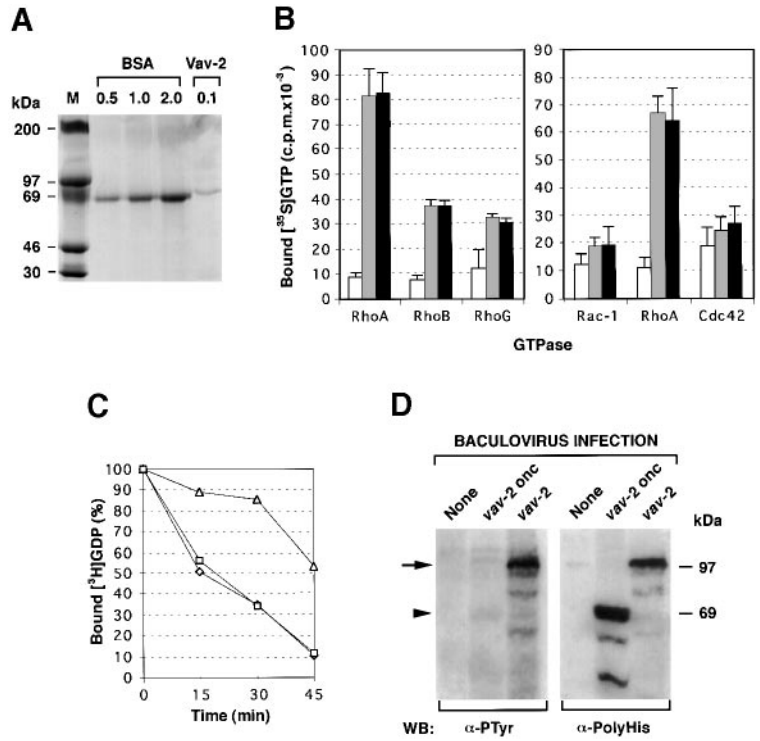

Fig. 5. (**A**) Purification of Vav-2 oncoprotein by chromatography on nickel beads. M, molecular weight markers. The amount of loaded proteins is given in μg. (**B**) Exchange activity of Vav-2 oncoprotein on Rho proteins. The indicated GDP-loaded GTPases were incubated for 45 min with [^{35}S]GTP-γS in the presence of phosphorylated Vav-2 oncoprotein (black boxes), non-phosphorylated Vav-2 oncoprotein (gray boxes) or autophosphorylated GST–Lck (white boxes) and the exchange obtained under each condition determined using a filter immobilization assay. (**C**)[^{3}H]GDP release assay of RhoA with phosphorylated Vav-2 oncoprotein (squares), non-phosphorylated Vav-2 oncoprotein (diamonds) and autophosphorylated GST–Lck (triangles). In (B), values represent the mean and SD of three (left panel) and four (right panel) independent determinations each performed in duplicate. (C) shows a representative experiment of two independent determinations, each performed in duplicate. (**D**) Immunoblot analysis using anti-phosphotyrosine (α-PTyr) or anti-polyhistidine (α-PolyHis) antibodies of total cell lysates derived from Sf9 cells infected with the indicated baculovirus. The migration of wild-type and oncogenic Vav-2 proteins is indicated by an arrow and an arrowhead, respectively.

the above proteins lacking the complete the C-terminal SH3–SH2–SH3 domains, the region involved in the interaction of Vav with protein tyrosine kinases (Bustelo, 1996). As shown in Figure 6A, the removal of the complete SH3–SH2–SH3 region from either the wild-type (plate 4) or the originally described oncogenic version of Vav(Δ1–67) (plate 5) results in the abrogation of their transforming activity. However, the same deletion in the Vav(Δ1–187) mutant yields a protein with still high oncogenic potential (2704 foci/μg; Figure 6A, plate 6). Anti-phosphotyrosine immunoblots of Vav immunoprecipitates obtained from two independent clones (X4-42 and X4-43) of Vav(Δ1–187 + Δ608–845)-transformed cells confirmed that this transforming version of Vav is not tyrosine phosphorylated *in vivo* (Figure 6B, left panel). As a positive control for the immunoblot, the anti-phosphotyrosine antibodies did recognize the Vav(Δ1–187) protein immunoprecipitated from two independent clones (X4-21 and X4-23) of transformed cells (Figure 6B, left panel). Western blot analysis with an anti-Vav antiserum confirmed that the Vav(Δ1–187 + Δ608–845) protein was present in the selected cell clones (Figure 6B, right panel).

As expected from the *in vitro* GDP/GTP exchange assays, the lack of requirement for a functional SH2 domain for the transforming activity of the Vav(Δ1–187) deletion mutant is also conserved in the *vav-2* oncogene, because a mutated form of this oncoprotein lacking a functional SH2 and the C-terminal SH3 domain [Vav-2(Δ1–186 + Δ718–868)] retains high levels of transforming activity when compared with the Vav-2(Δ1–186) oncogene (Figure 6A, plates 7 and 8). Taken together, these results demonstrate that the full oncogenic activation of Vav family members requires the elimination of both the CH and AD regions, a mutagenic event that produces Vav proteins with phosphorylation-independent GDP/GTP exchange activity.

The Vav-2 oncoprotein cooperate with RhoA subfamily proteins in cellular transformation

Co-expression of GEFs with their biological substrates leads to a synergistic response in cellular transformation (Bustelo *et al*., 1994; Quilliam *et al*., 1994). To confirm the role of Vav-2 as a Rho GEF *in vivo*, we tested the ability of wild-type members of the Rho/Rac family to cooperate with the Vav-2 oncoprotein in focus formation assays. To this end, the *vav-2* oncogene was transfected at suboptimal concentrations (100 ng) into NIH-3T3 cells either alone or in combination with an excess amount (600 ng) of the indicated GTPases, and the resulting foci of transformed cells were scored 15 days post-transfection. As expected, the expression of wild-type Rho GTPases in rodent fibroblasts resulted in no detectable transformation even after culturing the confluent cells for long periods of time (Figure 7A, and data not shown). Instead, the transfection of the *vav-2* oncogene in NIH-3T3 cells resulted in the induction of a low but detectable number

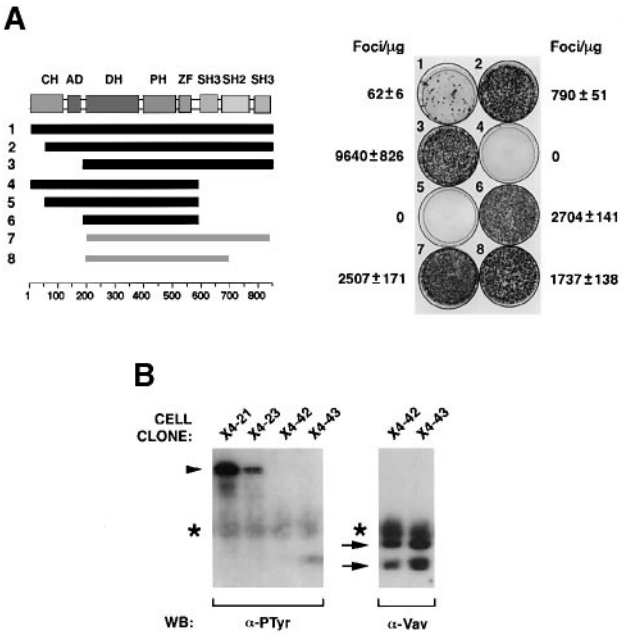

Fig. 6. (**A**) Oncogenic potential of Vav and Vav-2 truncated proteins. Left panel: highlighted domains of Vav family proteins include the calponin homology (CH), the acidic domain (AD), the Dbl homology (DH) region, the pleckstrin homology (PH) domain, zinc finger (ZF) and SH2 and SH3 domains. The Vav and Vav-2 proteins tested in focus formation assays are indicated by closed black and gray boxes, respectively. Amino acid numbers are indicated at the bottom. Right panel: transforming activity of each construct as determined by focus formation assay in NIH-3T3 cells. The amounts of expression vector used in these transfections were 1 μg (plates 1, 2, 4 and 5), 0.5 μg (plates 6, 7 and 8) or 0.1 μg (plate 3). Values represent the mean and SD of three independent transfections each performed in duplicate and are given as number of foci/μg of transfected DNA. The figure shows the Giemsa staining of the tissue culture plates of a representative focus assay. (**B**) Anti-Vav (α-Vav) and anti-phosphotyrosine (α-PTyr) immunoblot analysis of Vav immunoprecipitates obtained from cells expressing Vav(Δ1–187) or Vav(Δ1–187 + Δ608–845). The migration of Vav(Δ1–187) and Vav(Δ1–187 + Δ608–845) proteins is indicated by arrowheads and arrows, respectively. The asterisks indicate the migration of the immunoglobulin heavy chain. The bands of faster mobility observed in Vav(Δ1–187 + Δ608–845) immunoprecipitates are probably due to a cryptic start site activated upon deletion of *vav* cDNA sequences.

of foci (67.5 ± 16.2) of morphologically transformed cells that could be readily seen 6–8 days post-transfection (Figure 7A). Co-transfection of *rhoA* with *vav-2* led to a further increase (6.5-fold) in the number of foci induced by this oncogene (Figure 7A). Such cooperativity was not observed when the Vav-2 oncoprotein was co-expressed with $RhoA^{Q63L}$, a mutant version of RhoA with reduced GTPase activity which is bound preferentially to GTP (Figure 7B), further suggesting that this cooperativity is mediated by an activator–substrate relationship rather than the convergence of two independent signaling pathways. As a positive control for these transfections, we took advantage of the synergism observed for H-Ras with Vav family members (Bustelo *et al*., 1994) and $RhoA^{Q63L}$ (Khosravi-Far *et al*., 1995). As shown in Figure 7B, both Vav-2 and $RhoA^{Q63L}$ synergize with wild-type H-Ras in focus formation assays, resulting in highly enlarged foci that display Ras-like morphologies (Figure 7B, and data not shown). We also found that the *vav-2* oncogene and $RhoA^{Q63L}$ synergized with suboptimal concentrations of the H-*ras* oncogene, suggesting that this cooperativity is due to the cross-talk of two independent signaling pathways (data not shown). Interestingly, the *vav* oncogene also cooperates with wild-type and oncogenic H-*ras*, although this synergism produces foci with a Vav-like morphology (Bustelo *et al*., 1994).

In addition to wild-type RhoA, a small synergistic response (2.7-fold) was also observed when *vav-2* was co-transfected with *rho*B (Figure 7A, right panel). In contrast, no cooperativity was found when *vav-2* was co-transfected with expression vectors encoding wild-type Rac-1, RhoC, RhoG or Cdc42 proteins (Figure 7A, right panel). As a positive control, we conducted focus formation assays with the constitutively active forms of these GTPases to demonstrate that they were transforming when shifted to their GTP-bound state. $Rac\text{-}1^{Q61L}$, $RhoA^{Q63L}$, $RhoB^{Q63L}$ and $RhoC^{Q63L}$ were capable of inducing moderate levels of cellular transformation (Figure 7C), while $Cdc42^{Q61L}$ led to the appearance of single, multinucleated cells scattered throughout the cell monolayer (Figure 7C, and data not shown). As expected (Roux *et al*., 1997), transfection of NIH-3T3 cells with the constitutively active form of RhoG resulted in the appearance of a very low number of small foci (31 ± 17 foci/μg DNA; Figure 7C). Thus, with the exception of RhoG, the data from the cooperativity experiments *in vivo* correlate well with the enzyme specificity of Vav-2 observed *in vitro*. Given the low transforming activity of RhoG, it is possible that this GTPase could play an ancillary role in Vav-2 function distinct from proliferation-related responses (i.e. cytoskeletal organization).

Transient expression of the Vav-2 oncoprotein leads to morphological change in NIH-3T3 cells

Since the morphology of *vav-2*-transformed cells shown in Figure 1 could not be correlated unequivocally with the changes induced by any particular GTP-binding protein, we decided to eliminate all the epistatic events derived from the generation of oncogenically transformed cells by investigating the effect of transiently expressed Vav-2 oncoprotein in the cytoskeletal organization of NIH-3T3 cells. To this end, we used a liposome transfection technique to introduce saturating amounts (2 μg) of the *vav-2* oncogene into NIH-3T3 cells. For comparison, we also included in these transfections the *vav*(Δ1–67) and *dbl* oncogenes. In addition, those plasmids were co-transfected with suboptimal concentrations (250 ng) of a mammalian expression vector containing the humanized version of the green fluorescent protein (GFP) to recognize the cells that have integrated the exogenous DNA. At 24 h after transfection, cells were fixed, incubated with rhodamine-labeled phalloidin to visualize the actin network and finally subjected to microscopy analysis.

These experiments indicated that the expression of the Vav-2 oncoprotein leads to the induction of lamellipodia and pronounced membrane ruffling in NIH-3T3 cells. However, these cells show no obvious filopodia or stress fiber formation (Figure 8C and D). The expression of the Vav(Δ1–67) oncoprotein gives rise to a similar morphological change (Figure 8A and B). In contrast, the transient expression of the Dbl oncoprotein, a GEF specific for RhoA, RhoB, RhoC, RhoG and Cdc42 (Cerione and Zheng, 1996), leads to the generation of loosely attached,

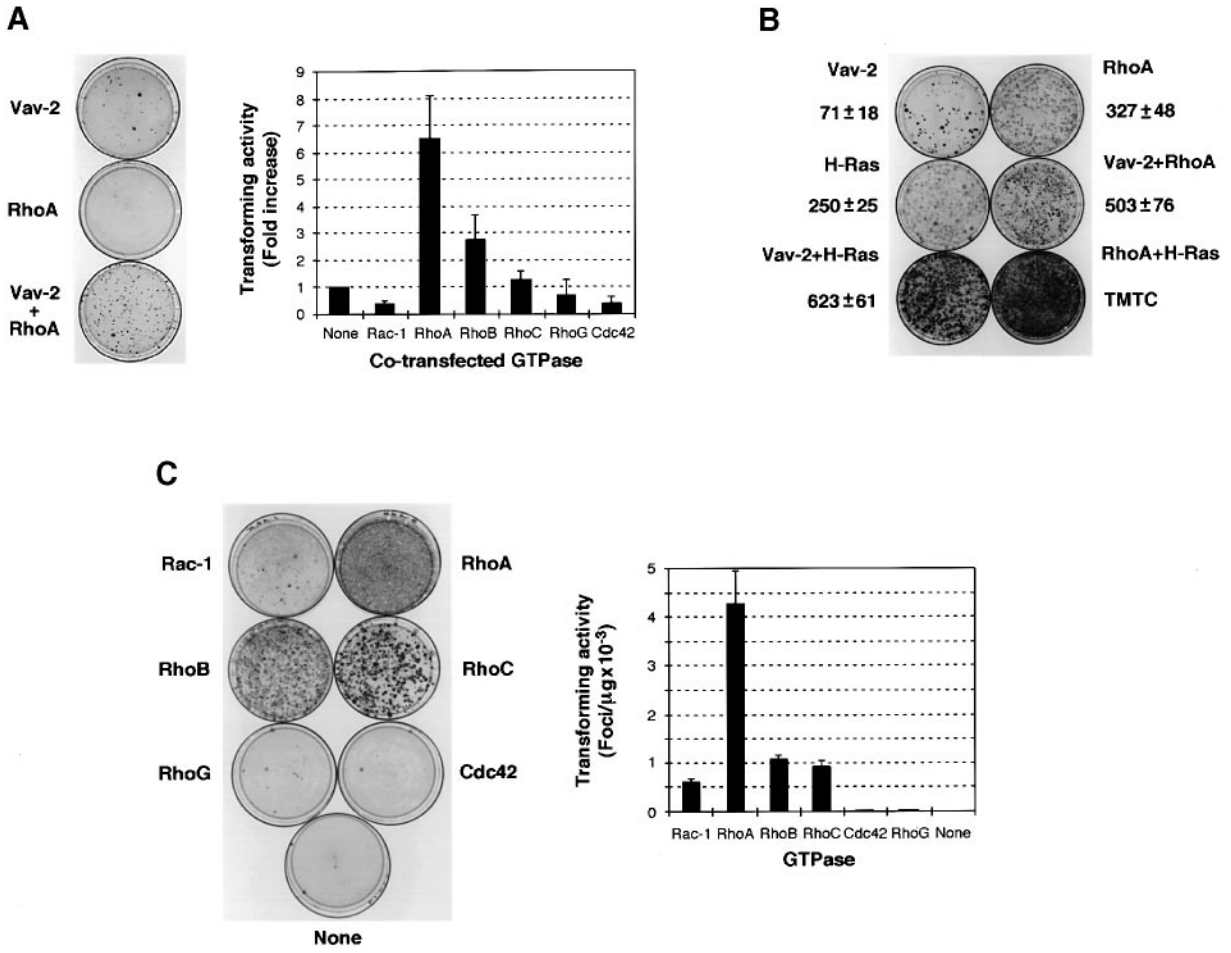

Fig. 7. (**A**) Cooperativity of Vav-2 oncoprotein with RhoA and RhoB GTPases. A plasmid containing the *vav-2* oncogene (100 ng) was co-transfected with vectors encoding the indicated GTPases (600 ng) and foci of transformed cells scored 15 days after transfection. Values in the right panel represent the mean and standard deviation of four independent experiments performed in duplicate, and are expressed as fold increase over the foci obtained with *vav-2* alone. (**B**) Cooperativity of $RhoA^{Q63L}$ and Vav-2 oncoprotein with wild-type H-Ras. Plasmids containing the *vav-2* oncogene (100 ng), *rho*A^{Q63L} (75 ng) and H-*ras* (300 ng) were introduced into NIH-3T3 cells in the indicated combinations and foci scored 15 days after transfection. TMTC, too many to count. (**C**) Transforming activity of constitutively active mutants of the Rho family. Cells were transfected with either 500 ng ($Rac\text{-}1^{Q61L}$, $RhoA^{Q63L}$, $RhoB^{Q63L}$ and $RhoC^{Q63L}$) or 1 µg ($RhoG^{Q61L}$ and $Cdc42^{Q61L}$) of expression vectors and foci scored after 15 days. In (B) and (C), values represent the mean and standard deviation of three independent transfections each performed in duplicate, and expressed as foci/10 cm plate (B) or foci/µg of transfected DNA (C). In (A–C), the pictures show the Giemsa staining of the tissue culture plates of a representative focus assay.

highly refringent rounded cells that project multiple filopodia from the plasma membrane (Figure 8E and F).

To correlate this morphological change with the function of members of the Rho family, we also transfected NIH-3T3 cells with the constitutively active mutants of various members of the Rho family. The expression of $RhoA^{Q63L}$ (Figure 8I and J), $RhoB^{Q63L}$ (K and L) and $RhoC^{Q63L}$ (M and N) generates rounded cells in which filopodia are absent. This morphology is similar to the rounded cells found in foci derived from the transfection of these GTP-binding proteins in rodent fibroblasts (data not shown). These shape changes are probably due to the contraction of the cortical actomyosin system, as previously described in other cell types (Jalink *et al*., 1994; Gebbink *et al*., 1997). In the case of $RhoB^{Q63L}$ and $RhoC^{Q63L}$, ~25% of these cells also show membrane blebbing, suggesting that some portion of these transfected cells have initiated an apoptotic process (data not shown). Under these transfection conditions, no induction of stress fiber formation was observed for any of the RhoA subfamily members (Figure 8I–N). The expression of $Cdc42^{Q61L}$ gives rise to a Dbl-like phenotype, with rounded, refractile cells that project multiple filopodia from the plasma membrane (Figure 8Q and R). These cells also show low levels (~10%) of membrane blebbing (Figure 8Q, and data not shown), an effect not observed in Dbl-transfected cells. Finally, the expression of activated mutants of Rac-1 (Figure 8G and H) or RhoG (O and P) induces some membrane ruffling and promotes the formation of lamellipodia that are significantly larger than those observed in Vav- and Vav-2-containing cells. Expression of the humanized GFP generates no obvious morphological change in the transfected cells (data not shown, and Figure 10A and B). Interestingly, we have found that in similar transfections in COS-1 cells, Vav-2, Dbl, $Rac\text{-}1^{Q61L}$ and $RhoG^{Q61L}$ (but not $RhoA^{Q63L}$ or $Cdc42^{Q61L}$) induce generalized membrane ruffling (data not shown). Taken together, these results indicate that the morphological change induced by Vav-2 and Vav activity resembles, although is not identical to, the activation of RhoG and/or Rac-1 in short-term assays

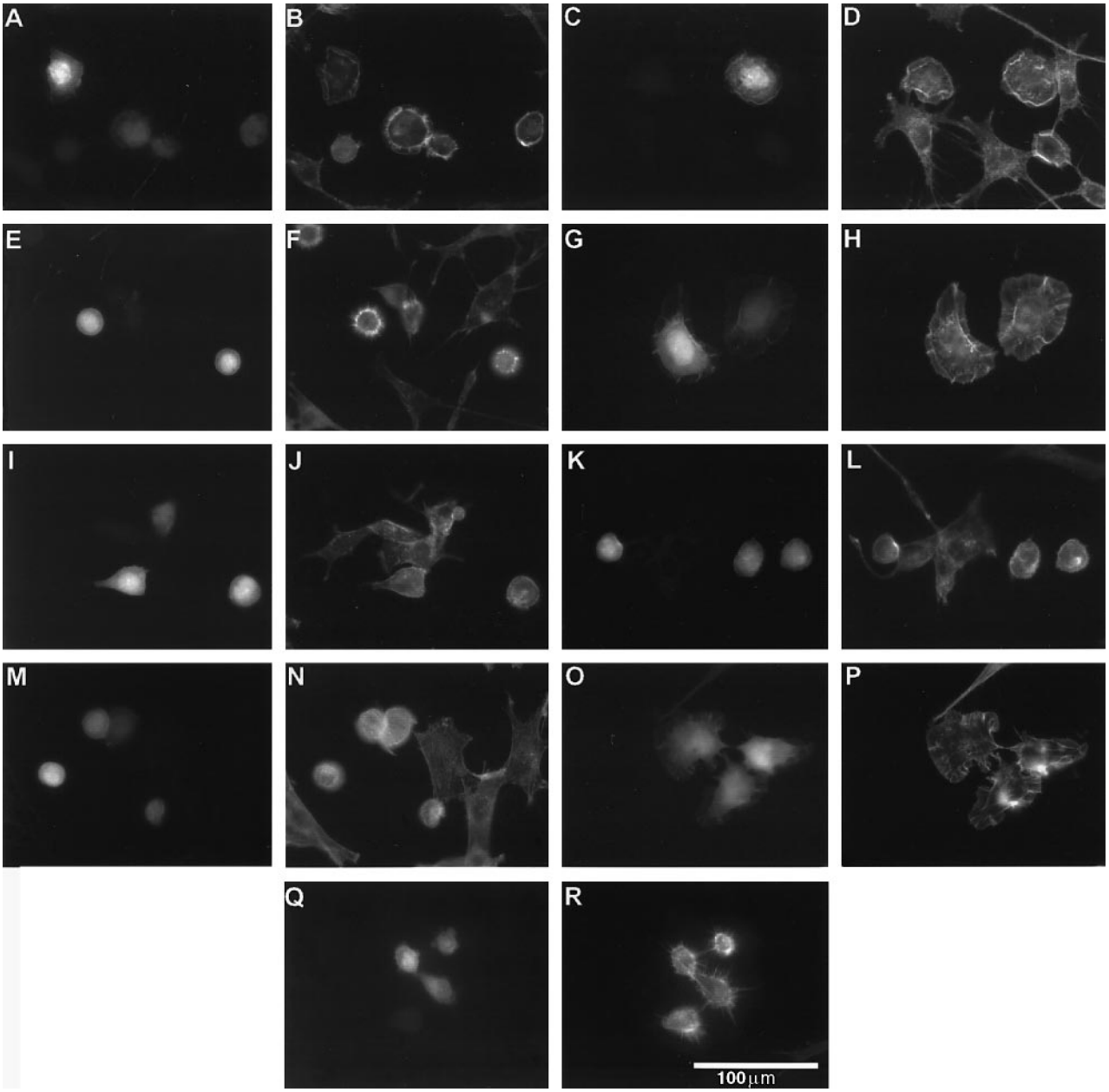

Fig. 8. Morphological change induced in NIH-3T3 cells by transient expression of DH and Rho family members. Cells were transfected with plasmids encoding the humanized GFP (A–R) plus the vectors containing the *vav*(Δ1–67) oncogene (**A** and **B**), the *vav-2* oncogene (**C** and **D**), the *dbl* oncogene (**E** and **F**) or constitutively active mutants of Rac-1 (**G** and **H**), RhoA (**I** and **J**), RhoB (**K** and **L**), RhoC (**M** and **N**), RhoG (**O** and **P**) and Cdc42 (**Q** and **R**). After 24 h, cells were fixed, stained with rhodamine–phalloidin and subjected to microscopy analysis with filters to visualize the fluorescence derived from the GFP (A, C, E, G, I, K, M, O and Q) or the rhodamine–phalloidin (B, D, F, H, J, L, N, P and R).

in different cell backgrounds. In contrast, Dbl promotes phenotypes similar to those triggered by the activation of Cdc42 and Rac-1/RhoG proteins in a cell type-dependent manner.

Activation of wild-type Vav-2 in vivo by tyrosine phosphorylation

It has been reported previously that the *vav-2* proto-oncogene lacks transforming activity in rodent fibroblasts (Schuebel *et al*., 1996). In agreement with these observations, we found that wild-type Vav-2 could not synergize with RhoA even at saturating concentrations of DNA (Figure 9, and data not shown). We therefore decided to investigate whether the activity of the *vav-2* proto-oncogene product could be enhanced by tyrosine phosphorylation. To this end, we first determined the ability of a constitutively active form of Lck (Y505F mutation) to induce the activation of wild-type Vav-2 by conducting focus formation assays with all the possible combinations of *vav-2*, lck^{Y505F} (100 ng each) and wild-type *rho*A (700 ng). As shown in Figure 9, neither Vav-2, Lck^{Y505F} nor RhoA showed any transforming activity when expressed alone. Likewise, no transformation is induced when *rho*A is co-transfected with either *vav-2* or lck^{Y505F}. Instead, co-transfection of wild-type *vav-2* with lck^{Y505F} leads to a pronounced oncogenic response that is enhanced further by the inclusion of saturating concentrations of *rho*A (Figure 9). As in the case of the oncogenic version, the

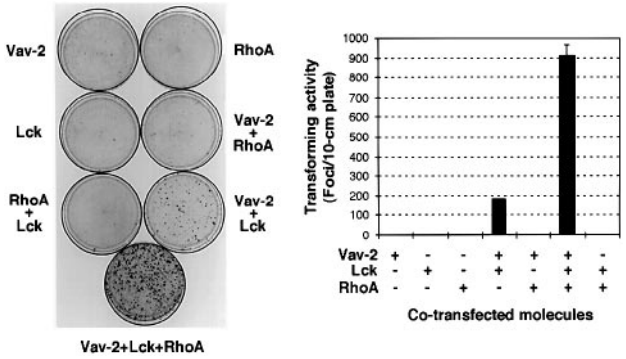

Fig. 9. Cooperativity of wild-type Vav-2 with Lck^{Y505F} and/or RhoA. Cells were co-transfected with the indicated constructs and foci scored 15 days after transfection. Values represent the mean and SD of three independent experiments each performed in duplicate. The left panel shows the Giemsa staining of tissue culture plates from a representative transfection experiment.

morphology of the *vav-2* proto-oncogene-transformed cells is different from those obtained by co-expressing wild-type Vav and Lck^{Y505F} (data not shown).

As a second test to demonstrate the activation of wild-type Vav-2 protein by tyrosine phosphorylation *in vivo*, we also investigated the possible Lck-dependent stimulation of wild-type Vav-2 in transient transfection assays in NIH-3T3 cells. For this purpose, we transfected these cells with suboptimal concentrations of a GFP-containing vector either alone or in combination of a 4-fold excess of expression vectors containing the *vav-2* proto-oncogene and/or the lck^{Y505F} mutant. Cells were cultured for 24 h in the presence of the liposome–DNA mix, fixed, stained with rhodamine–phalloidin and observed under the microscope. As shown in Figure 10, the expression of GFP (A and B) or wild-type Vav-2 (E and F) results in no lamellipodia or membrane ruffling induction in these culture conditions. Likewise, the transient expression of GFP with Lck^{Y505F} in NIH-3T3 cells generates no detectable membrane ruffling, although these cells consistently display dendrite-like projections from the cell body (Figure 10C and D). The co-transfection of lck^{Y505F} with the *vav-2* proto-oncogene induces both lamellipodia and membrane ruffles similar to those observed in co-transfections of the oncogenic version of Vav-2 and, less frequently, a rounding up of the transfected cells similar to that observed in cells expressing activated RhoA subfamily proteins (Figure 10G and H). Interestingly, the $LckY^{505}F$/Vav-2 co-expressing cells lack the dendrite-like projections characteristic of cells expressing Lck^{Y505F} alone, suggesting that the Lck-specific effect is mediated by a signaling molecule whose function is antagonized by the activation of conventional Rho family pathways (Figure 10G and H). These results highlight the important role of tyrosine phosphorylation for the activation of the wild-type Vav-2 and the implication of Rho proteins in the mitogenic and cytoskeletal pathways of both wild-type and oncogenic versions of this GEF.

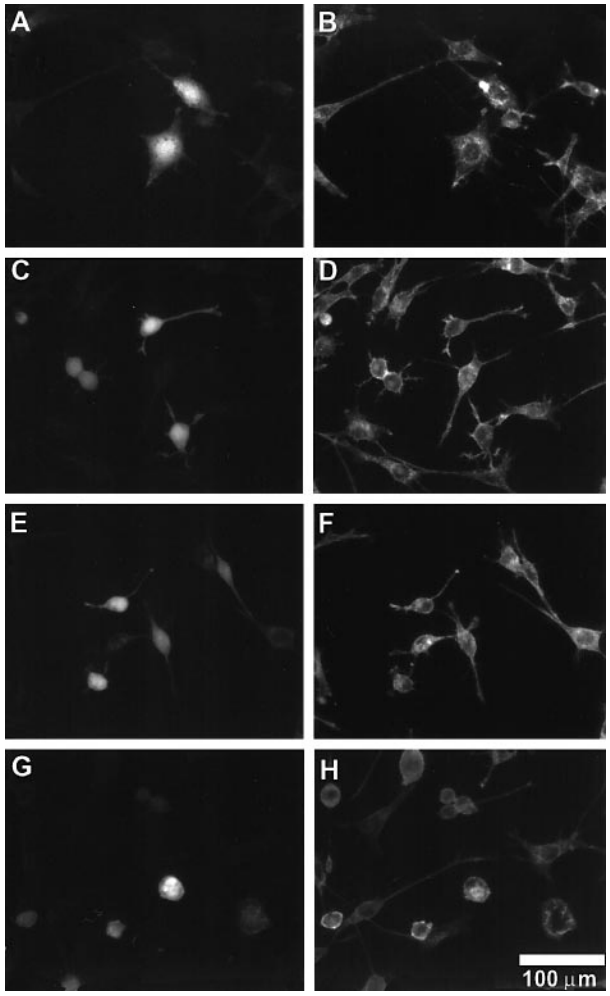

Fig. 10. Morphological change induced in NIH-3T3 cells by transient expression of Lck^{Y505F} and wild-type Vav-2 proteins. Cells were transfected with plasmids encoding the humanized GFP alone (**A** and **B**), GFP plus lck^{Y505F} (**C** and **D**), GFP plus the *vav-2* proto-oncogene (**E** and **F**) and with the three combined vectors (**G** and **H**). After 24 h, cells were fixed, stained with rhodamine–phalloidin, and subjected to microscopy analysis with filters to visualize the fluorescence derived from GFP (A, C, E and G) or the rhodamine–phalloidin (B, D, F and H).

Discussion

In this work, we provide evidence showing that Vav-2, a novel member of the Vav family of oncoproteins, is a phosphorylation-dependent GEF with specificity towards the RhoG and the RhoA subfamily. In contrast, Vav-2 lacks enzyme activity on other structurally related GTPases, such as Rac-1, Rac-2, RhoC and Cdc42. Using the same batch of GTP-binding proteins, we have found that tyrosine-phosphorylated Vav targets preferentially Rac-1, Rac-2 and RhoG (Crespo *et al.*, 1997, and unpublished observations). The common use of RhoG by Vav and Vav-2 is not entirely surprising, since the primary structure of this Rac-related GTPase is the most closely related to Rho proteins. Altogether, these biochemical studies indicate that Vav family proteins are activated by a common post-translational modification but utilize overlapping, but not identical, subsets of GTP-binding proteins.

The functional relationship of Vav-2 and RhoA subfamily members is reinforced further by mitogenic assays *in vivo*. We have shown that the co-expression of the *rho*A proto-oncogene with suboptimal concentrations of the *vav-2* oncogene leads to a 6-fold increase in the transformation response, as determined by focus formation assays in NIH-3T3 cells. This value is similar to the

cooperativity found (5-fold) in co-transfections of the TC21 GTP-binding protein with its bona fide exchange factor, Ras GRF (data not shown). Instead, the Vav-2 oncoprotein did not cooperate with the constitutively active form of RhoA, further suggesting that Vav-2 is acting upstream of this GTPase in a linear signaling pathway. By co-transfecting the *vav-2* oncogene with representative members of the Rho/Rac family, we have also found that such a synergistic response is in good agreement with the enzyme specificity found for Vav-2 *in vitro*. The only exception was RhoG, a GTPase whose nucleotide exchange is enhanced by Vav-2 but that does not cooperate with *vav-2* in cell transformation. This discrepancy is probably due to the specialization of RhoG in cell processes not strictly correlated with the regulation of the mitogenic status of cells. In agreement with this possibility, the Rho^{GQ61L} mutant displays a very low transforming activity in rodent fibroblasts (<35 foci/μg DNA). These foci are composed of only a very few cells, and do not grow in size even after prolonged periods of time. This contrasts with the transforming activity of all the other Rho family members tested, whose transforming activity ranged from 500 foci (Rac-1) to ~5000 foci (RhoA) when equivalent amounts of expression vector were used. Despite this lack of transforming activity, we have shown that the constitutively active mutant of RhoG can induce other cellular responses, including Rac-1-like morphological changes in NIH-3T3 cells within short periods of time (24 h). RhoG also activates other biological responses such as the stimulation of JNK (data not shown). These observations suggest that the role of RhoG in Vav-2 transformation is more likely to be circumscribed to the regulation of morphological change rather than to the modulation of cell proliferation.

The multiple engagement of GTP-binding proteins by the Vav-2 oncoprotein may be the cause of the complex morphological change observed in *vav-2*-transformed but not in *vav*-transformed cells. This morphology is also difficult to correlate with the activation of any GTP-binding protein known so far. For instance, *vav-2*-transformed cells are frequently multinucleated and show unusually large cell areas, a phenotype that cannot be observed in any NIH-3T3 cell line expressing the constitutively active mutants of Rac-1, RhoA, RhoB, RhoC or Cdc42. $Cdc42^{Q61L}$ does induce enlarged and multinucleated cells, but they usually remain isolated in the cell monolayer and never develop foci of transformed cells, probably due to a permanent arrest in the G_2/M phase. In addition, cultures of $Cdc42^{Q61L}$-expressing cells obtained by antibiotic selection do not sustain such a continuous generation of multinucleated and giant cells as that observed in *vav-2*-transformed cell lines. The morphology of the *vav-2*-induced foci could not be reproduced even when paired combinations of these GTP-binding proteins were co-transfected in focus formation assays. However, consistent with the hypothesis of the multiple engagement of GTP-binding proteins by the Vav-2 oncoprotein, we did observe that the expression of the *dbl* oncogene, an oncogene encoding a GEF for RhoA, RhoB, RhoC, RhoG and Cdc42 (Zheng *et al*., 1995), results in the generation of foci with a morphology indistinguishable from those induced by the *vav-2* oncogene.

The transient transfection assays conducted in the presence of Vav-2 and Dbl have also shown an interesting cell type-specific hierarchy in the activation of their substrates. Thus, even though Dbl can bind to Rac-1 and can activate the nucleotide exchange on RhoA, RhoB, RhoC, RhoG and Cdc42 *in vitro* (Zheng *et al*., 1995), its transient expression in NIH-3T3 and COS-1 cells elicits morphological phenotypes resembling those induced by the activation of Cdc42 and Rac-1/RhoG, respectively. Similarly, expression of the *vav-2* oncogene induces predominantly membrane ruffling and filopodia even though its protein product can also activate RhoA and RhoB GTPases *in vitro*. Thus, it is possible that the activation of Cdc42 overrides (or inhibits) the morphological signals mediated by Rho and RhoG while, in its absence, Rac-1 and/or RhoG override the rounding up of cells characteristic of RhoA, RhoB and RhoC expression. In favor of this hypothesis, it has been shown that the expression of activated Rac-1 leads to a PAK-dependent inactivation of Rho cytoskeletal effects (Lim *et al*., 1996). Alternatively, the specific effects elicited by Vav-2 and Dbl oncoproteins can also reflect differences in the protein levels and/or the kinetics of the biological responses of the endogenous Rho family proteins targeted by those exchange factors. Given the extensive cross-talk among Rho GTPases (Hall, 1998), the cell-type-specific responses of Dbl in NIH-3T3 and COS-1 cells may be the consequence of the different levels of engagement by Cdc42 of either its direct effectors or the downstream Rac-1 protein, leading to filopodia formation in NIH-3T3 cells and to Rac-1-derived responses in COS-1 cells. Further studies using pair-wise combinations of each of these GTP-binding proteins in a number of cell types will allow all these possibilities to be distinguished.

The *in vivo* experiments shown in this study have also illustrated the important role that tyrosine phosphorylation plays in the activation of Vav proteins. Unlike its oncogenic version, the *vav-2* proto-oncogene lacks transforming activity even when used at saturating concentrations and under the regulation of strong viral promoters such as the MMTV long terminal repeat (Schuebel *et al*., 1996; this work). However, when this proto-oncogene is co-transfected with a protein tyrosine kinase, transformation levels as high as those found with similar concentrations of the *vav-2* oncogene can be detected. Such a transforming response can be enhanced ~6-fold further by co-transfecting *rho*A-containing vectors, further supporting the role of this GTPase in the Vav-2 mitogenic pathway. The role of phosphorylation of Vav-2 activity is confirmed further by the Lck-dependent morphological change induced by wild-type Vav-2 in transient transfection assays in NIH-3T3 cells.

A feature common to most Rho/Rac GEFs, including the Vav family, is their oncogenic activation by N-terminal truncation (for a review see Cerione and Zheng, 1996). Despite this common mutagenic event, very few studies have addressed the mechanism by which such truncations lead to the constitutive activation of Rho/Rac GEFs. To date, only a single study has shown that the wild-type and oncogenic versions of Dbl display identical kinetics of GDP/GTP exchange activity *in vitro*, suggesting that the Dbl N-terminal domain regulates the activity of this GEF *in trans* (Zheng *et al*., 1995). In the case of Vav-2, we have found that its oncogenic form can stimulate the same

spectrum of GTPases as the wild-type version. However, the Vav-2 oncoprotein does not require the prior phosphorylation on tyrosine residues to display full enzyme activity, indicating that the oncogenic activation of the *vav-2* oncogene correlates with the expression of a truncated, constitutively active protein whose function is independent of upstream regulatory signals. This appears to be a general stimulatory mechanism for Vav family members, as we have found that a similar deletion of the CH domain and AD of Vav also leads to the generation of a Vav protein that is highly transforming, even in the absence of detectable levels of tyrosine phosphorylation.

The use of truncated Vav proteins has identified not only the mechanism for full oncogenic activation of Vav family proteins but also the minimal structural requirements for Vav transformation. Thus, we have found that a truncated Vav protein containing exclusively the DH, PH and zinc finger regions displays high levels of transforming activity (≈2000 foci/μg transfected plasmid). This minimal transforming version of Vav is reminiscent of the structure of many Rho/Rac GEFs that contain a DH/PH region and, occasionally, a zinc finger (Cerione and Zheng, 1996). Further deletions or point mutations in those three domains totally disrupt Vav transformation (N.Movilla and X.R.Bustelo, manuscript in preparation), indicating that the PH and zinc finger regions play essential roles in Vav function. Recent reports have indicated that the binding of phospholipids to the Vav PH domain enhances both the phosphorylation of Vav and its phosphorylation-dependent exchange activity, at least *in vitro* (Han *et al*., 1998). Because the truncated Vav protein (Δ1–187 +Δ608–845) is not tyrosine phosphorylated *in vivo*, our results suggest that both the PH and zinc finger regions should also influence Vav function in processes independent of phosphorylation. Whether those regions are involved in the modulation of the GDP/GTP exchange activity of Vav, subcellular localization or unrelated effector functions remains to be determined.

Collectively, our results establish the Vav family as a group of GEFs intimately associated with the signaling of protein tyrosine kinases. Perhaps more importantly, the finding that Vav and Vav-2 display different enzyme specificities suggests a signaling model by which membrane receptors with associated tyrosine kinase activity will be capable of inducing distinct physiological responses by modulating the kinetics of phosphorylation of, or physical association with, Vav proteins specific for different Rho/Rac molecules. Because the Rac-1-specific Vav protein is expressed preferentially in the hematopoietic system (Bustelo, 1996), our results imply that there may be other members of the Vav family specific for Rac-1 in non-hematopoietic cells. The isolation and biochemical characterization of these new putative members of the Vav family will contribute to a better understanding of the signals responsible for triggering the cytoskeletal and nuclear responses observed in proliferating cells.

Materials and methods

Plasmids

Baculoviruses were generated from either pVL1393 derivatives in the case of mouse Vav protein (pAZ12; Bustelo *et al*., 1994), pAcHLT derivatives (Pharmingen) in the case of the mouse wild-type (pKES8) and oncogenic (residues 189–868) Vav-2 proteins (pKES32) and a pFASTBAC-derivative (Gibco-BRL) in the case of oncogenic Dbl protein (pNM12). GST fusion proteins were expressed in bacteria using pGEX derivatives encoding GST–Rac-1 (pXRB98), GST–RhoA (pXRB96), GST–RhoB (pXRB157) and GST–Cdc42 (pXRB94). GST–RhoG was expressed using the pCEV30G-RhoG plasmid provided by T.Miki (National Institutes of Health, Bethesda, MD). For focus formation assays, the mouse *vav-2* proto-oncogene (pXRB138) (Schuebel *et al*., 1996), *vav-2* oncogene (pXRB141) (Schuebel *et al*., 1996), *vav-2*(Δ1–186 + Δ718–868) (pKES52), wild-type mouse *vav* (pJC11) (Coppola *et al*., 1991), *vav*(Δ1–67) (pJC12) (Coppola *et al*., 1991), *vav*(Δ1–187) (pKES12), *vav*(Δ608–845) (pNM1), *vav*(Δ1–67 + Δ608–845) (pKES20), *vav*(Δ1–187 +Δ608–845) (pKES21) and human *dbl* oncogene (pNM3) were cloned in the pMEX expression vector. For transient expression experiments in mammalian cells, the mouse *vav-2* proto-oncogene (pAO1), *vav-2* oncogene (pAO2), *vav*(Δ1–67) oncogene (pcDNAoncovav) (Crespo *et al*., 1997) and *dbl* oncogene (pcDNAoncdbl) were constructed in pcDNA derivatives. Wild-type *rho*B (pXRB51), *rho*B oncogene (pXRB159), wild-type *rho*C (pXRB52) and *rho*C oncogene (pXRB160) were cloned in the pCEFL-AU5 expression vector. Mammalian expression vectors encoding wild-type and constitutively active mutations of Rac-1, RhoA and Cdc42 were pCEFL-AU5 derivatives provided by J.S.Gutkind (National Institutes of Health, Bethesda, MD). The mammalian expression vector encoding Lck^{Y505F} (pcDNA derivative) and those containing the wild-type and constitutively active RhoG (pCEFL-AU5 derivative) proteins were gifts from P.Crespo (Departamento de Biología Molecular, Universidad de Cantabria, Santander, Spain). The vector encoding the humanized version of GFP (pEGFP-C1) was purchased from Clontech.

Protein purification

Exponentially growing Sf9 cells were infected at 2×10^6 cells/ml with the appropriate high-titer baculovirus supernatant at a multiplicity of infection of 5–10. After 48 h, cells were harvested by centrifugation and washed twice with ice-cold phosphate-buffered saline solution (PBS, Gibco-BRL), and final cell pellets were kept frozen at –70°C. For purification, cell pellets were thawed on ice and lysed with 10 mM Tris–HCl pH 7.5, 150 mM NaCl, 1% Triton X-100, 1 mM phenylmethylsulfonyl fluoride (PMSF), 1 mM orthovanadate, 10 mM NaF, 5 mM imidazole (Sigma) and 10% glycerol. After clearing the cell lysates by centrifugation at 35 000 r.p.m. for 30 min at 4°C, supernatants were incubated with nickel beads (Talon™, Clontech) at 4°C for 2 h. Adsorbed proteins were washed three times in buffer A (20 mM Tris–HCl pH 7.4, 150 mM NaCl, 0.1% Triton X-100), twice in buffer B (20 mM Tris–HCl pH 7.4, 500 mM NaCl, 0.1% Triton X-100) and twice in buffer C (10 mM Tris–HCl pH 7.5, 150 mM NaCl). At that point, proteins were eluted in two steps by addition of 4 ml of 50 and 100 mM imidazole in 10 mM Tris–HCl pH 7.5, 150 mM NaCl and 10% glycerol. Aliquots of the fractions were analyzed by SDS–PAGE and those containing eluted proteins were pooled, dialyzed and concentrated by several centrifugation steps in Centriplus-30 vials (Amicon). Concentrated proteins were quantified by SDS–PAGE in the presence of known concentrations of bovine serum albumin (BSA) as standard and stored at –20°C. Dbl total cellular lysates were obtained from baculovirus-infected Sf9 cells exactly as described by Zheng *et al*. (1995). The purified GST-tagged Lck and Syk proteins purified from Sf9 cells were provided by Dr J.Fragnoli (Bristol-Myers Squibb Pharmaceutical Research Institute, Princeton, NY). GTP-binding proteins were purified from *Escherichia coli* as GST fusion proteins, according to standard procedures.

In vitro kinase, GDP/GTP exchange and GTPase assays

Kinase reactions with the appropriate protein tyrosine kinase were conducted for 30 min at room temperature in 20 mM Tris–HCl pH 7.5, 5 mM $MgCl_2$ with either 1 mM ATP for exchange reactions or, alternatively, with 20 μM ATP plus 2.5 μCi of [γ-^{32}P]ATP (Amersham) to obtain radiolabeled Vav-2. [^{35}S]GTP-γS incorporation and [^{3}H]GDP release assays were performed essentially as described by Hardt *et al*. (1998). Exchange reactions with Dbl total cell lysates were conducted as indicated by Zheng *et al*. (1995). For GTP hydrolysis assays, 0.55 μg of each purified GST–GTPase were incubated with [α-^{32}P]GTP for 1 h at 37°C and final products separated by thin-layer chromatography as described previously (Bollag and McCormick, 1995).

Transfection assays

NIH-3T3 cells (150 000 cells/10 cm plate) were transfected by the $CaPO_4$ precipitation method using 20 μg of calf thymus DNA (Boehringer Mannheim) (van der Eb and Graham, 1980). After 24 h, DNA/$CaPO_4$

precipitates were removed by two washes with Dulbecco's modified Eagle's medium (DMEM)/5% calf serum (Hyclone), and cultured in the same medium for 15 days. After this period, cells were fixed with formaldehyde and stained with Giemsa to count the foci of morphologically transformed cells. Foci of spontaneously transformed cells were not included in the final scores. All transfections were done in duplicate using non-linearized plasmids purified by ion-exchange chromatography (Qiagen). Generation of stable cell clones was performed by randomly picking individual foci with the aid of cloning cylinders followed by soft agar cloning. For transient transfection assays, NIH-3T3 or COS-1 cells were grown on uncoated coverslips in 3.5 cm plates (48 000 cells/plate) and transfected with the indicated plasmids for 24 h using the FuGENE 6 liposome method (Boehringer Mannheim) exactly as described by the commercial supplier. All cells were maintained in DMEM supplemented with 10% calf serum.

Immunofluorescence

Parental NIH-3T3 cells and cells transformed by the *vav-2* (B305-11-3-1) or the *vav* (B37-47) oncogene were seeded in serial dilutions onto collagen-coated coverslips, grown for 72 h in DMEM containing 10% calf serum, washed once with PBS and fixed with 4% paraformaldehyde. After two washes with PBS for 5 min each, cells were permeabilized with a 0.1% solution of saponin in PBS for 10 min. Cells were then washed three times in PBS (5 min each), blocked in a 1% solution of BSA in PBS for 1 h, and incubated with anti-vinculin antibodies (1:100 dilution in blocking solution, Sigma) for 2 h. Cells were incubated for 1 h with an anti-mouse secondary antibody coupled to Texas red (1:200 dilution, Amersham). Fluorescein isothiocyante (FITC)–phalloidin (Sigma) was added during the last 20 min of this incubation. Cells finally were washed five times (5 min each) with PBS, mounted onto microscope slides and visualized by microscopy. Alternatively, cells were incubated with either anti-vinculin (1 h) or FITC–phalloidin (Sigma) (20 min) alone and processed as described above. Immunofluorescence with anti-α-tubulin antibodies (Oncogene Sciences) was conducted on methanol-fixed cells following the steps indicated above. In the case of transient transfections, cells were washed twice with PBS, fixed with 3% paraformaldehyde, permeabilized with 0.1% Triton X-100 in PBS, and incubated with rhodamine–phalloidin (Molecular Probes) for 10 min. After three washes for 5 min each in PBS, the coverslips were mounted onto microscope slides using Slowfade (Molecular Probes). All steps were conducted at room temperature.

Acknowledgements

We thank Drs J.S.Gutkind, P.Crespo, J.C.Lacal and T.Miki for their gift of vectors, Dr M.Barbacid for the Vav-encoding pAZ12 baculovirus, and Dr J.Fragnoli for GST–Lck and GST–Syk. We also appreciate one of the anonymous referees whose comments significantly improved our manuscript. This work was made possible by a research grant from the US National Cancer Institute to X.R.B. (CA7373501) who is a Sinsheimer Scholar for Cancer Research.

References

Boguski,M.S. and McCormick,F. (1993) Proteins regulating Ras and its relatives. *Nature*, **366**, 643–654.

Bollag,G. and McCormick,F. (1995) Intrinsic and GTPase-activating protein-stimulated Ras GTPase assays. *Methods Enzymol.*, **255**, 161–170.

Bustelo,X.R. (1996) The VAV family of signal transduction molecules. *Crit. Rev. Oncogen.*, **7**, 65–88.

Bustelo,X.R. and Barbacid,M. (1992) Tyrosine phosphorylation of the *vav* proto-oncogene product in activated B cells. *Science*, **256**, 1196–1199.

Bustelo,X.R., Suen,K.-L., Leftheris,K., Meyers,C.A. and Barbacid,M. (1994) Vav cooperates with Ras to transform rodent fibroblasts but is not a Ras GDP/GTP exchange factor. *Oncogene*, **9**, 2405–2413.

Cerione,R.A. and Zheng,Y. (1996) The Dbl family of oncogenes. *Curr. Opin. Cell Biol.*, **8**, 216–222.

Coppola,J., Bryant,S., Koda,T., Conway,D. and Barbacid,M. (1991) Mechanism of activation of the *vav* protooncogene. *Cell Growth Differ.*, **2**, 95–105.

Crespo,P., Schuebel,K.E., Ostrom,A.A., Gutkind,J.S. and Bustelo,X.R. (1997) Phosphotyrosine-dependent activation of Rac-1 GDP/GTP exchange by the *vav* proto-oncogene product. *Nature*, **385**, 169–172.

Eva,A. and Aaronson,S.A. (1985) Isolation of a new human oncogene from a diffuse B-cell lymphoma. *Nature*, **316**, 273–275.

Gebbink,M.F., Kranenburg,O., Poland,M., van Horck,F.P., Houssa,B. and Moolenaar,W.H. (1997) Identification of a novel, putative Rho-specific GDP/GTP exchange factor and a RhoA-binding protein: control of neuronal morphology. *J. Cell Biol.*, **137**, 1603–1613.

Hall,A. (1998) Rho GTPases and the actin cytoskeleton. *Science*, **279**, 509–514.

Han,J. *et al*. (1998) Role of substrates and products of PI 3-kinase in regulating activation of Rac-related guanosine triphosphatases by Vav. *Science*, **279**, 558–560.

Hardt,W.D., Chen,L.M., Schuebel,K.E., Bustelo,X.R. and Galán,J.E. (1998) *S.typhimurium* encodes an activator of Rho GTPases that induces membrane ruffling and nuclear responses in host cells. *Cell*, **93**, 815–826.

Henske,E.P., Short,M.P., Jozwiak,S., Bovey,C.M., Ramlakhan,S., Haines,J.L. and Kwiatkowski,D.J. (1995) Identification of VAV2 on 9q34 and its exclusion as the tuberous sclerosis gene *TSC1*. *Ann. Hum. Genet.*, **59**, 25–37.

Jalink,K., van Corven,E.J., Hengeveld,T., Morii,N., Narumiya,S. and Moolenaar,W.H. (1994) Inhibition of lysophosphatidate- and thrombin-induced neurite retraction and neuronal cell rounding by ADP ribosylation of the small GTP-binding protein Rho. *J. Cell Biol.*, **126**, 801–810.

Katzav,S., Cleveland,J.L., Heslop,H.E. and Pulido,D. (1991) Loss of the amino-terminal helix–loop–helix domain of the *vav* proto-oncogene activates its transforming potential. *Mol. Cell. Biol.*, **11**, 1912–1920.

Khosravi-Far,R., Solski,P.A., Clark,G.J., Kinch,M.S. and Der,C.J. (1995) Activation of Rac1, RhoA and mitogen-activated protein kinases is required for Ras transformation. *Mol. Cell. Biol.*, **15**, 6443–6453.

Lim,L., Manser,E., Leung,T. and Hall,C. (1996) Regulation of phosphorylation pathways by p21 GTPases. *Eur. J. Biochem.*, **242**, 171–185.

Quilliam,L.A., Huff,S.Y., Rabun,K.M., Wei,W., Park,W., Broek,D. and Der,C.J. (1994). Membrane-targeting potentiates CDC25 and SOS activation of Ras transformation. *Proc. Natl Acad. Sci. USA*, **91**, 8512–8516.

Roux,P., Gauthier-Rouviere,C., Doucet-Brutin,S. and Fort,P. (1997) The small GTPases Cdc42Hs, Rac1 and RhoG delineate Raf-independent pathways that cooperate to transform NIH3T3 cells. *Curr. Biol.*, **7**, 629–637.

Schuebel,K., Bustelo,X.R., Nielsen,D.A., Song,B.J., Barbacid,M., Goldman,D. and Lee,I.J. (1996) Isolation and characterization of murine *vav-2*, a member of the *vav* family of proto-oncogenes. *Oncogene*, **13**, 363–371.

Teramoto,H., Salem,P., Robbins,K.C., Bustelo,X.R. and Gutkind,J.S. (1997) Tyrosine phosphorylation of the *vav* proto-oncogene product links FcεRI to the Rac1–JNK pathway. *J. Biol. Chem.*, **272**, 10751–10755.

Van Aelst,L. and D'Souza-Chorey,C. (1997) Rho GTPases and signaling networks. *Genes Dev.*, **11**, 2295–2322.

van der Eb,A.J. and Graham,F.L. (1980) Assay of transforming activity of tumor virus DNA. *Methods Enzymol.*, **65**, 826–839.

Zheng,Y., Hart,M.J. and Cerione,R.A. (1995) Guanine nucleotide exchange catalyzed by *dbl* oncogene product. *Methods Enzymol.*, **256**, 77–84.

Received March 25, 1998; revised September 14, 1998; accepted September 15, 1998